

# Self-assembled nanostructures from amphiphilic globular protein–polymer hybrids

Qi Cao<sup>1</sup> · Naipu He<sup>1</sup> · Yue Wang<sup>1</sup> · Zhenwu Lu<sup>1</sup>

Received: 6 April 2017 / Revised: 27 August 2017 / Accepted: 31 August 2017 /  
Published online: 4 September 2017  
© Springer-Verlag GmbH Germany 2017

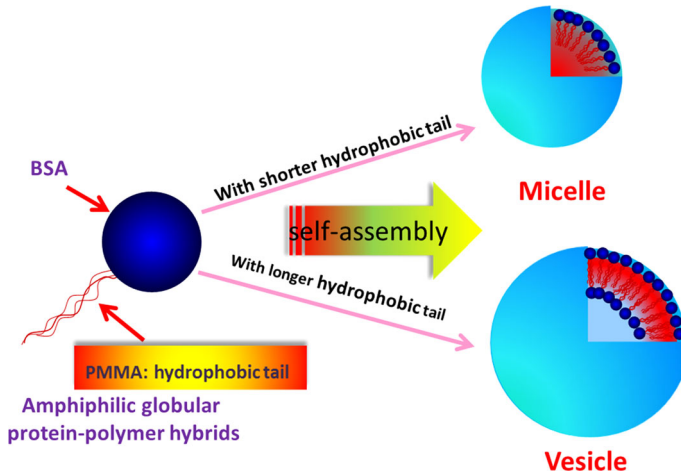
**Abstract** Amphiphilic globular protein–polymer hybrids, consisting of poly(methyl methacrylate) (PMMA) as hydrophobic tail and globular protein as hydrophilic head, are prepared by the end-functional PMMA covalently binding to the primary amino groups of bovine serum albumin (BSA) in the phosphate buffer saline (PBS)/acetone mixture solvents at pH 5. The self-assembly behaviors of amphiphilic BSA–PMMA hybrids are explored in aqueous solution by the dynamic light scatter (DLS), scanning electron microscopy (SEM) and transmission electron microscopy (TEM). The self-assembled morphologies of the amphiphilic BSA–PMMA hybrids are controlled by the length of hydrophobic PMMA chains. The amphiphilic BSA–PMMA hybrids with the longer hydrophobic PMMA chains self-assembled into spherical vesicles and elongated tubular vesicles, and conversely, they self-assembled into micelles. A vesicle consists of BSA as two outer hydrophilic layers and PMMA as hydrophobic wall.

---

✉ Naipu He  
henaipu@mail.lzjtu.cn

<sup>1</sup> College of Chemical and Biological Engineering, Lanzhou Jiaotong University, 88 Anning Xilu, Lanzhou 730070, China

**Graphical Abstract** Amphiphilic globular protein–polymer hybrids consist of PMMA as hydrophobic tail and globular protein BSA as hydrophilic head. Amphiphilic globular protein–polymer hybrids self-assembled into micelles or vesicles in phosphate buffer saline. The self-assembled morphology of amphiphilic protein–polymer hybrids was controlled by adjusting the length of hydrophobic chains.



**Keywords** Amphiphilic protein–polymer hybrids · Bovine serum albumin · Self-assembly · Vesicles · Micelles

## Introduction

Amphiphilic block copolymers have been largely explored during the last decades. This is due to the unique properties that arise from the incompatibility of the blocks, leading to a large number of different self-assembled structures in the bulk or in the selective solvents [1–4]. These self-assembled structures are the basis for applications including information storage, drug delivery and photonic materials [5–8]. Subsequently, another kind of novel amphiphilic block copolymers based on the large-sized “nanoatoms” such as fullerenes, polyhedral oligomeric silsesquioxane (POSS) and proteins as building blocks have been designed and synthesized [9, 10]. Because “nanoatoms” are well-defined molecular structure with different sizes, symmetry, surface groups and functions, they can be used as versatile nanobuilding blocks [11, 12]. In fact, these novel amphiphilic block polymer consisting of nanoatoms self-assembled into a large number of different nanostructures [13–17].

In globular proteins, the overall molecular shape and 3D conformation are held by the multiple secondary interactions between various residues of the polypeptide chain. The amino residues in the protein molecule can be modified to fabricate the protein–polymer hybrids (PPHs). In additional, the unique self-assembly feature of

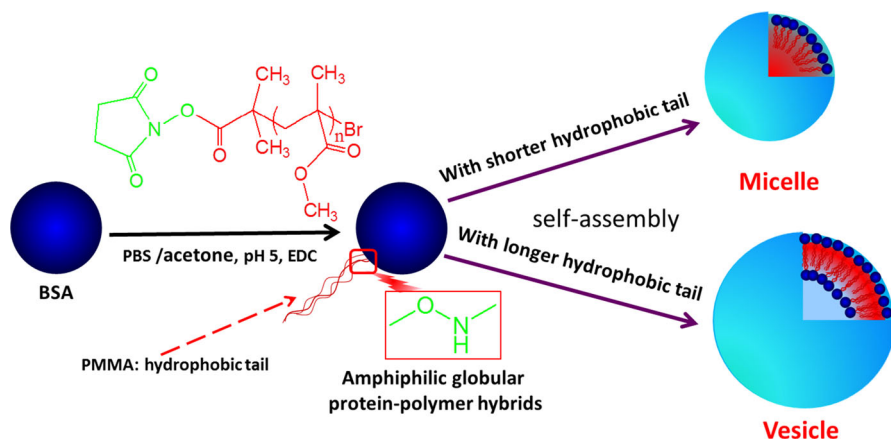
protein induced PPHs to self-assemble into desired nanostructures [18–20]. PPHs consisting of protein covalently linking to synthetic polymer have been previously designed and have significant applications in the area of material science and biomedicine because of the elegant functionalities and unique self-assembly characteristic [21, 22]. PPHs possess the advantages of both the biofunctional properties and the self-assembly characteristic of protein and the good stability, diversity and some other fascinating properties of the synthetic polymer [23, 24]. Moreover, PPHs can self-assemble into a wide range of nanostructures such as micelles, micellar rods, and vesicles [25, 26]. For instance, amphiphilic PPHs consisting of an enzyme lipase B as hydrophilic head covalently connected to a single hydrophobic polymeric tail polystyrene (PS) can be induced to self-assemble in a fashion similar to that of small amphiphilic molecules [27]. mCherry–pNIPAAm hybrids self-assembled into the highly disordered lamellae or hexagonally perforated lamellae depending upon the selectivity of the solvent during evaporation [28–30]. Amphiphilic BSA–PCL hybrids displayed the excellent self-assembly behaviors to form vesicles and micelles [31]. As a result, their self-assembly is anticipated to exhibit features of both small molecules and traditional macromolecules or lead a new self-assembly pattern, and is emerging as a fascinating research field [32, 33]. Especially, the self-assembled materials have protein-specific functions such as fluorescence or catalytic activity [34–36].

In our previous works, PPHs with hydrophilic polymer were successfully prepared by the “grafting-to” method [37, 38]. These PPHs self-assembled into different nanostructures in the aqueous solutions and the self-assembly behaviors were controlled by pH and temperature. In the current work, amphiphilic globular protein–polymer hybrids consisting of poly(methyl methacrylate) (PMMA) as hydrophobic tail and globular protein bovine serum albumin (BSA) as hydrophilic head are fabricated. The purpose is to explore their self-assembly behaviors in the aqueous solution. It is focused on that the length of hydrophobic tail effected on the self-assembly morphology of amphiphilic globular protein–polymer hybrids. PMMA with an activated end group (NHS–PMMA) were prepared by the atom transfer radical polymerization (ATRP). The coupling reaction was carried out using *N*-ethyl-*N*-(3-dimethylaminopropyl) carbodiimide hydrochloride (EDC) as a couple reagent in phosphate buffer saline (PBS)/acetone mixture solvents at pH 5 (Scheme 1).

## Experimental section

### Materials

Bovine serum albumin (BSA, FM67000) was obtained from Shanghai Bio Life Science & Technology Co., Ltd. Methyl methacrylate (MMA) was purchased from Tianjin Kaixin Chemical Technology Co., Ltd. Cuprous bromide ( $\text{Cu}^{\text{I}}\text{Br}$ ) was purchased from Tianjin Guangfu Institute of Superfine Chemical Industry. MMA and CuBr were further purified before use. 2-Bromoisobutyric acid (BIBA, 98%), *N,N,N',N'',N'''*-pentamethyl diethylenetriamine (PMDETA) and *N,N*-dimethylformamide (DMF, >99.5%) were obtained from Aladdin. *N*-ethyl-*N*-(3-



**Scheme 1** Fabrication and self-assembly of amphiphilic BSA–PMMA hybrids

dimethylaminopropyl) carbodiimide hydrochloride (EDC), *N*-hydroxysuccinimide (NHS), acrylamide, bisacrylamide, *N,N'*-tetramethylethylenediamine (TEMED), glycine, glycerol, bromophenol blue, tris(hydroxymethyl) aminomethane (Tris), ammonium persulfate (APS), dithiothreitol (DTT), sodium dodecyl sulfate (SDS), coomassie brilliant blue G-250, the molecular weight standard and regenerated cellulose membranes were purchased from Shanghai Sangon Biological Engineering Technology & Services Co., Ltd. All other reagent grade chemicals were obtained from local suppliers and used without further treatment. Phosphate buffer saline (PBS) was prepared using the distilled water.

### Synthesis of ATRP initiator (NHS ester)

ATRP initiator, 2-bromoisobutanoic acid *N*-hydroxysuccinimide ester, was synthesized by EDC-mediated condensation of NHS and 2-bromoisobutyric acid (BIBA) in dichloromethane ( $\text{CH}_2\text{Cl}_2$ ). The preparation of ATRP initiator has been reported in our previous paper [37].  $^1\text{H}$ NMR ( $\text{CDCl}_3$ , ppm): 2.856 (4H, t,  $-\text{CH}_2-$ , succ.), 2.063 (6H, s,  $-\text{CH}_3$ ).

### Preparation of the end-functional poly(methyl methacrylate) (NHS-PMMA) by ATRP

ATRP initiator, 2-bromoisobutanoic acid *N*-hydroxysuccinimide ester, was employed to initiate atom transfer radical polymerization of methyl methacrylate (MMA). In detail, 0.052 g (0.36 mmol) of cuprous bromide ( $\text{Cu}^{\text{I}}\text{Br}$ ) and 75  $\mu\text{L}$  (0.36 mmol) of PMDETA were added into a 100 mL round-bottom flask with a magnetic stir bar. The solution was purged with nitrogen gas for five times. Then MMA and 8 mL of acetone were added. After stirring for 10 min, 0.102 g (0.36 mmol) of ATRP initiator was added. Polymerization process was conducted with constant stirring for 24 h at 45 °C under an atmosphere of nitrogen. The

resulting liquid was purified through a column of neutral alumina and the solvent was removed under reduced pressure. The polymer was precipitated by methanol and then filtered. The polymer with an activated end group, NHS–PMMA, was collected as a white powder. In the work, functional PMMA molecules with two different molecular weights were prepared by ATRP. The molecular weights of PMMA were controlled by adjusting the molar ratio of monomer to initiator. The data was listed in the Table 1.

### Preparation of globular amphiphilic protein–polymer hybrids

BSA solution at a concentration of  $6 \times 10^{-6}$  mol/L was prepared in phosphate buffer saline (PBS) at pH 5.0. EDC (6.0 mg;  $3 \times 10^{-5}$  mol) was added to 5 mL of BSA solution. The given NHS–PMMA was completely dissolved in acetone and then added into BSA solution. The reaction mixtures were gently stirred for 10 h under an atmosphere of nitrogen in darkness. The resulting solution was dialyzed for three times in dialysis bag (cutoff, MWCO 25 kDa) against PBS to remove the unreacted residues and acetone for 3 days in total at room temperature in darkness. The aqueous solutions of amphiphilic BSA–PMMA hybrids were stored at 4 °C for further use.

### Characterization

$^1\text{H}$ NMR spectra of samples were obtained using a Bruker DMX 400 NMR spectrometer with  $\text{CDCl}_3$  as solvents. GPC analysis was carried out with GPC 2000 (Waters, USA) using THF as eluents at a flow rate of  $1.0 \text{ mL min}^{-1}$  at 35 °C. PS calibration kit was used as the calibration standard. The particle size and distribution of samples were measured using a dynamic light scattering (DLS) equipment (Nano ZS, Malvern, UK) at 25 °C with a 633 nm He–Ne laser at a scattering angle of 90°. Transmission electron microscopy (TEM) was performed on a JEM-1200EX microscope [Japan Electron Optics Lab. Co. LTD. (JEOL), Tokyo, Japan]. The sample solutions, on a copper grid with suspended carbon films, were dried at room temperature and stained with 0.25% phosphotungstic acid. Scanning electron microscopy (SEM) studies were conducted using a JSM-6701F scanning electron

**Table 1** The molecular weights and polydispersities of the end-functional poly(methyl methacrylate) (PMMA) synthesized by ATRP

PMMA <sup>a</sup>	Initiator (mmol)	Monomer (mmol)	$M_n$		$M_w/M_n$ (GPC <sup>c</sup> )	Conversion (%)
			Theory <sup>b</sup>	GPC <sup>c</sup>		
PMMA <sub>33</sub>	0.36	36	3784	3568	1.4	35.2
PMMA <sub>80</sub>	0.36	72	7224	8306	1.4	34.8

<sup>a</sup> All reactions carried out with  $[\text{CuBr}]:[\text{initiator}]:[\text{PMDETA}] = 1:1:1$ , under an atmosphere of nitrogen for 24 h at 45 °C

<sup>b</sup>  $M_n$  (theory) =  $\frac{m [\text{MMA}]}{n [\text{initiator}]} \times \text{conversion} (\%) + M [\text{initiator}]$

<sup>c</sup> GPC analysis was carried out with GPC using THF as eluents at a flow rate of  $1.0 \text{ mL min}^{-1}$  at 35 °C

microscope [Japan Electron Optics Lab. Co. LTD. (JEOL), Tokyo, Japan]. A droplet of sample solution was directly dropped on a silicon wafer, followed by air drying under the ambient condition.

### Sodium dodecyl sulfate polyacrylamide gel electrophoresis (SDS-PAGE)

Five percent condensation gel and 8% separation gel were prepared at room temperature using the standard concentration of acrylamide, bisacrylamide, SDS, APS and TEMED. All samples were diluted using a buffer solution (2×) consisting of Tris–HCl at pH 6.8, bromophenol blue, SDS, DTT and glycerol, and then incubated at 100 °C. After the gel was completely gelled, the reference BSA and the samples were loaded into the wells. Electrophoresis was carried out using a vertical electrophoresis apparatus (DYY, Beijing, China). The electrode buffer contained 25 mmol/L tricine and 250 mmol/L glycine at pH 8.3. The condensation gel was run at 100 V and the current was limited to 15 mA using DYY-12C-type electrophoresis power supply (DYY, Beijing, China). When samples were within the separation gel, the voltage was increased to 500 V and the current was limited to 15 mA. Electrophoresis duration was typically around 4 h at 5 °C. The gel was stained by 0.1% (w/v) coomassie brilliant blue R-250 solution at 40 °C for 4 h. Stained gels were destained with shaking constantly until the band of stained sample was clearly visible. The final gel was scanned by the scanner.

## Results and discussion

### Preparation of the end-group PMMA (NHS–PMMA)

As shown in Scheme 1, the end-functional PMMA (NHS–PMMA) was synthesized using 2-bromoisobutanoic acid *N*-hydroxysuccinimide ester as a ATRP initiator and CuBr/*N,N,N',N'',N'''*-pentamethyl diethylenetriamine (PMDETA) as the catalyst/ligand systems by ATRP in acetone solution. In the present paper, the end group of NHS–PMMA would covalently bind to the primary amino groups of BSA. It was confirmed by <sup>1</sup>HNMR that the activity end group was introduced in the resulting polymer PMMA (Fig. 1). <sup>1</sup>HNMR(400 MHz, CDCl<sub>3</sub>), δ (ppm): 0.75–1.31 (m, 9H, –CH<sub>3</sub>), 1.76–2.11 (m, 2H, –CH<sub>2</sub>–), 2.82 (s, 4H, –CH<sub>2</sub>–, succ), 3.60 (m, 3H, –O–CH<sub>3</sub>).

ATRP is a facile way to incorporate an initiator site into a molecule leading to a wide range of functionalized polymers. ATRPs were commonly used to introduce the reactive group in the resulting polymer [39–42]. It facilitates the covalent binding of protein to the end group of polymer.

The molecular weights of the end-functional poly(methyl methacrylate) (PMMA) were controlled by adjudging the molar ratio of monomer to initiator (Table 1). The amount of initiator was kept at 0.36 mmol, and the molar ratio of monomer to initiator was changed by the amount of monomer. All reactions carried out with [CuBr]:[initiator]:[PMDETA] = 1:1:1, under an atmosphere of nitrogen for 24 h at 45 °C. The molecular weight of PMMA was determined by GPC (Fig. 2). It was found from GPC plot that the PMMA with different molecular weight, i.e.,

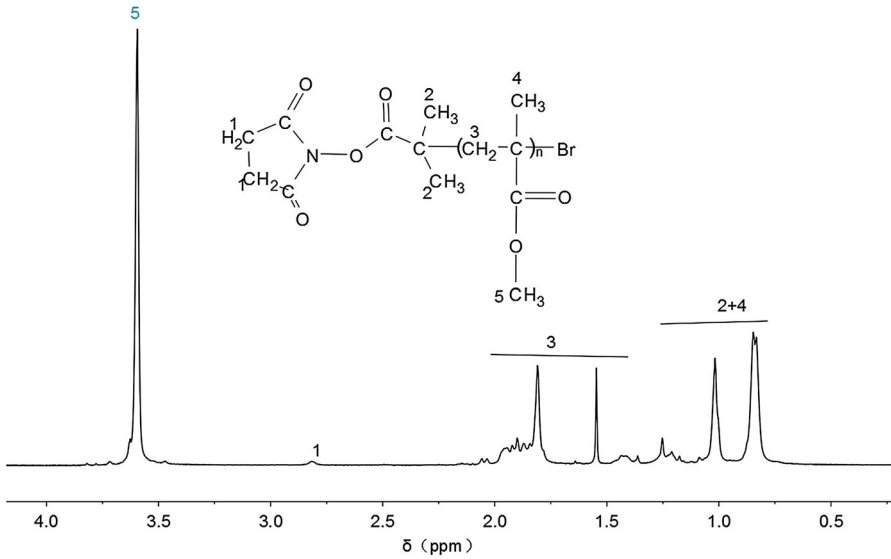


**Fig. 1**  $^1\text{H NMR}$  spectrum of the end-functional PMMA

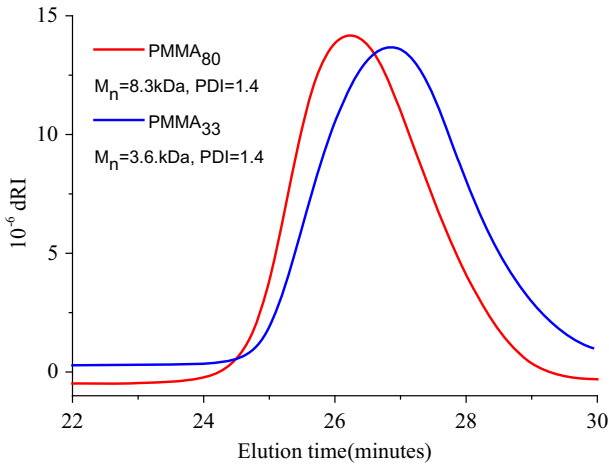


**Fig. 2** GPC plot of PMMA

PMMA<sub>33</sub> ( $M_n = 3.6$  kDa, PDI = 1.4), and PMMA<sub>80</sub> ( $M_n = 8.3$  kDa, PDI = 1.4) were prepared. All PMMA samples have a narrow molecular weight distribution, but with lower monomer conversion ( $\sim 35\%$ ). Separation of polymers is based on size exclusion by GPC. As shown in Fig. 2, PMMA with the higher molecular weight has a shorter retention time, and conversely, it has a longer retention time.

## Preparation of globular amphiphilic protein–polymer hybrids by “grafting-to” method

The amino group of protein was always used as an available site covalently binding to the carboxylic group to form new amide bonds [43–45]. BSA was completely dissolved in phosphate buffer saline (PBS) in advance. Because PMMA could not dissolve in PBS, PMMA was completely dissolved in acetone. Consequently, as Scheme 1 shows, the end-functional PMMA (NHS-PMMA) covalently bind to the primary amino of BSA using EDC as a coupling reagent in PBS/acetone mixture (PBS:acetone = 25:1) at pH 5 at room temperature. The molar ratio of BSA to PMMA was fixed at 1:10. The resulting solutions were purified and isolated by dialysis.

The BSA–PMMA hybrids were characterized by SDS-PAGE (Fig. 3). The molecular weight standard protein (Lane Marker) and the native BSA (Lane BSA) were used as references. The electrophoretic band of BSA was observed in Lane BSA in accordance with the position at 66.2 kDa in Lane Marker. Lane 1 and Lane 3 in Fig. 3 present the SDS-PAGE of BSA–PMMA<sub>33</sub> hybrids and BSA–PMMA<sub>80</sub> hybrids. Compared with native BSA, some native BSA appeared at 66 kDa which are the unmodified native BSA, which indicated that the native proteins were not completely modified and retained in the protein hybrids. And some moved slower than the native BSA, which suggested the higher molecular weight BSA hybrids were prepared. The results revealed that some proteins were grafted by PMMA. In the experimental, the resulting solution was dialyzed for three times in dialysis bag

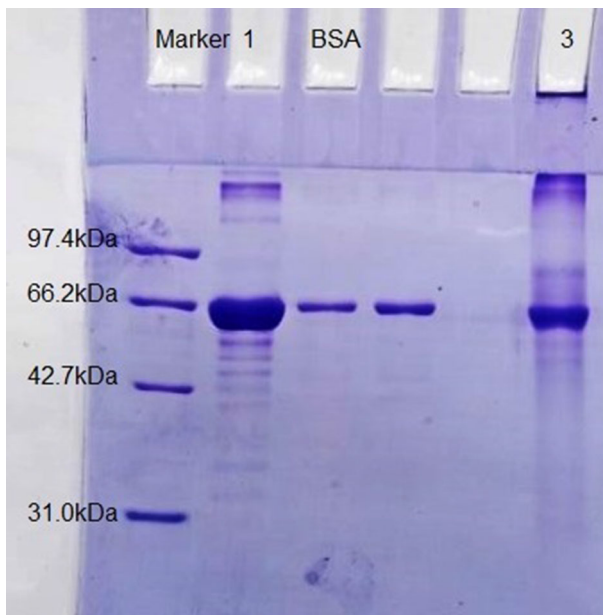


**Fig. 3** SDS-PAGE of native BSA and BSA–PMMA hybrids



(cutoff, MWCO 25 kDa) against PBS to remove the unreacted polymer. In addition, the reaction of polymer linking to protein is a low efficiency, which is a common and unavoidable challenge in similar literature [31, 46, 47].

Meanwhile, the protein content of BSA–PMMA<sub>80</sub> hybrid electrophoretic band was higher than that of BSA–PMMA<sub>33</sub> hybrids. In addition, it can be found that some BSA–PMMA<sub>80</sub> hybrid electrophoretic band protein hybrids did not migrate and retained in the well. It is due to BSA linking to PMMA with the higher molecular weight, leading to lower solubility of BSA–PMMA<sub>80</sub> hybrids. In the SDS-PAGE experiment, it is well known that charge density, the molecular weight and solubility of protein affected the electrophoretic migration of protein. As a result, the molecular weight of PMMA affected the electrophoretic migration.

### Self-assembly of amphiphilic BSA–PMMA hybrids in aqueous solution

Their self-assembly behaviors of amphiphilic BSA–PMMA hybrids with different length of hydrophobic PMMA chain, consisting of BSA as hydrophilic block and PMMA as hydrophobic block, were investigated by DLS and TEM in PBS at pH 7.4. The DLS results (Fig. 4) showed that the average diameter of BSA–PMMA<sub>33</sub> hybrids and BSA–PMMA<sub>80</sub> hybrids was 100 and 350 nm, respectively. The diameter of nanoparticles increased with the increase of the PMMA molecular weight, which may be due to the length of the hydrophobic PMMA chains. As shown in SEM images (Fig. 5), BSA–PMMA<sub>33</sub> hybrids self-assembled into separated nanoparticles with uniform size. Meanwhile, BSA–PMMA<sub>80</sub> hybrids self-assembled into nanoparticles with irregular size, and nanoparticles were gathered together.

The TEM images revealed that micelles and vesicles were obtained (Fig. 6). BSA–PMMA<sub>33</sub> hybrids self-assembled into spherical micelles with a diameter of 50–100 nm (Fig. 6a). In contrast, BSA–PMMA<sub>80</sub> hybrids self-assembled into spherical vesicles with a diameter of 100–400 nm (Fig. 6b) and elongated tubular vesicles (Fig. 6c). It may be due to the longer length of hydrophobic PMMA chains. It has been proposed that amphiphilic polymers with the longer hydrophobic chains tend to form vesicles, and conversely, they favor micelle formation [48–51]. These

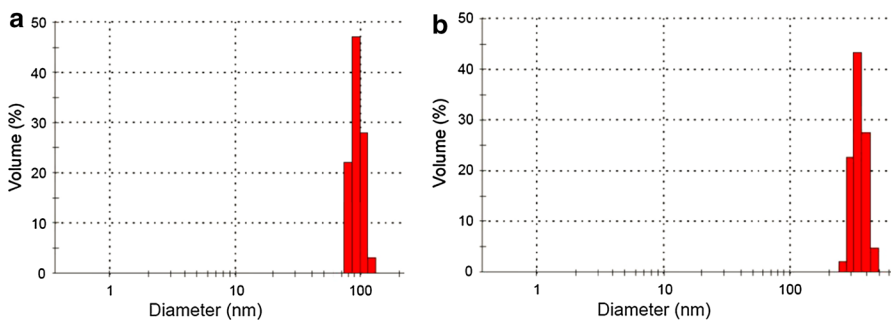


**Fig. 4** The DLS results of amphiphilic globular protein–polymer hybrids with different length of hydrophobic PMMA chains **a** BSA–PMMA<sub>33</sub> hybrids and **b** BSA–PMMA<sub>80</sub> hybrids

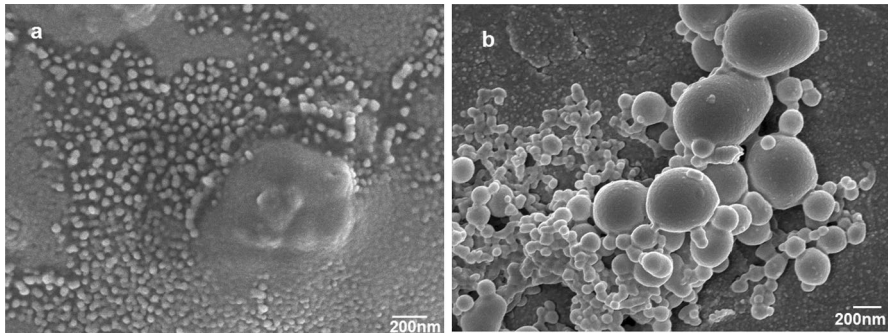


**Fig. 5** Scanning electron microscopy (SEM) images of **a** nanoparticles self-assembled by BSA-PMMA<sub>33</sub> hybrids and **b** nanoparticles self-assembled by BSA-PMMA<sub>80</sub> hybrids in aqueous solution

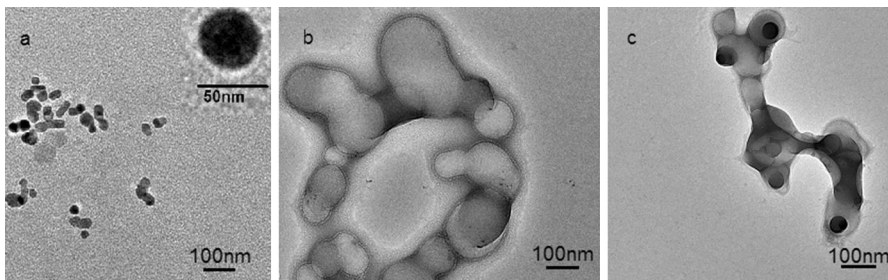


**Fig. 6** Transmission electron microscopy (TEM) images of **a** micelles self-assembled by BSA-PMMA<sub>33</sub> hybrids and **b, c** vesicles self-assembled by BSA-PMMA<sub>80</sub> hybrids in aqueous solution

results suggested that the self-assembled morphology of amphiphilic BSA-PMMA hybrids may be controlled by adjusting the length of PMMA.

BSA, a globular protein, is a typical polyampholyte and has hydrophilic surface in aqueous solution. PMMA is hydrophobic linear in aqueous solution. Amphiphilic BSA-PMMA hybrids consist of PMMA as hydrophobic tail and globular protein BSA as hydrophilic head. The structure of amphiphilic BSA-PMMA hybrids was similar to that of traditional amphiphilic block copolymers and small molecule surfactants [48–51]. It was proposed that vesicle consists of BSA as two outer hydrophilic layers and PMMA as a hydrophobic wall.

In our previous works, double hydrophilic protein-polymer hybrids self-assembled into a few vesicles in aqueous solution at the lower pH. Temperature-responsive protein-polymer hybrids self-assembled into separate spherical nanoparticles below the LCST of PPHs, in contrast, bundles and clusters were observed above the LCST of PPHs [37, 38]. In the current paper, hydrophobic PMMA was employed to form amphiphilic protein-polymer hybrids. Compared with double hydrophilic protein-polymer hybrids, the self-assembly morphology of amphiphilic protein-polymer hybrids distinguished from that of double hydrophilic protein-polymer hybrids. Because of BSA-PMMA hybrids consisting of PMMA as hydrophobic tail and globular protein BSA as hydrophilic head, the self-assembly

behavior of amphiphilic protein–polymer hybrids represented the unique properties of amphiphilic block copolymers.

## Conclusions

In summary, we have fabricated a series of amphiphilic globular protein–polymer hybrids consisting of PMMA as hydrophobic tail and globular protein BSA as hydrophilic head by the “grafting-to” method. Amphiphilic globular protein–polymer hybrids with different length of hydrophobic PMMA chains self-assembled into micelles or vesicles. BSA–PMMA hybrids with the longer hydrophobic PMMA chains self-assembled into spherical vesicles and elongated tubular vesicles. The various nanostructures will be expected to be used as a controlled drug delivery and other biomaterials.

**Acknowledgements** We gratefully acknowledge the National Natural Science Foundation of China (21164003) for financial support.

## Compliance with ethical standards

**Conflict of interest** The authors declare that they have no conflict of interest.

## References

1. Maynard HD (2013) Proteins in a pill. *Nat Chem* 5:557–558
2. Schacher FH, Rupar PA, Manners I (2012) Functional block copolymers: nanostructured materials with emerging applications. *Angew Chem Int Ed* 51:7898–7921
3. Carlsen A, Lecommandoux S (2009) Self-assembly of polypeptide-based block copolymer amphiphiles. *Curr Opin Colloid Interface Sci* 14:329–339
4. Riess G (2003) Micellization of block copolymers. *Prog Polym Sci* 281:107–1170
5. Feng A, Yuan J (2014) Smart nanocontainers: progress on novel stimuli-responsive polymer vesicles. *Macromol Rapid Commun* 35:767–779
6. Salimi E, Ghaee A, Ismail AF, Othman MHD, Sean GP (2016) Current approaches in improving hemocompatibility of polymeric membranes for biomedical application. *Macromol Mater Eng* 301:771–800
7. Liu Y, Liu Y, Yin J-J, Nie Z, Ruan Z (2015) Self-assembly of amphiphilic block copolymer-tethered nanoparticles: a new approach to nanoscale design of functional materials. *Macromol Rapid Commun* 36:711–725
8. Tang Z, He C, Tian H, Ding J, Hsiao BS, Chu B, Chen X (2016) Polymeric nanostructured materials for biomedical applications. *Prog Polym Sci* 60:86–128
9. Raffa P, Wever DAZ, Picchioni F, Broekhuis AA (2015) Polymeric surfactants: synthesis, properties, and links to applications. *Chem Rev* 11:8504–8563
10. Zhang WB, Yu X, Wang CL, Sun HJ, Hsieh IF, Li Y, Dong XH, Yue K, Horn RV, Cheng SZD (2014) Molecular nanoparticles are unique elements for macromolecular science: from “nanoatoms” to giant molecules. *Macromolecules* 4:1221–1239
11. Zhang W, Chu Y, Mu GY, Eghtesadi SA, Liu YC, Zhou Z, Lu XL, Kashfipour MA, Lillard RS, Yue K, Liu TB, Cheng SZD (2017) Rationally controlling the self-assembly behavior of triarmed POSS–organic hybrid macromolecules: from giant surfactants to macroions. *Macromolecules* 50:5042–5050
12. Rusen E, Marculescu B, Preda N, Bucur C, Mihut L (2008) Synthesis and optical properties of water-soluble poly(vinylpyrrolidone)-modified fullerene C<sub>60</sub>. *Polym Bull* 61:581–592
13. He N, Wang R (2012) Self-assembly of protein with polymer. *Prog Chem* 24:94–100

14. Xu Y, Chen M, Xie J, Li C, Yang C, Deng Y, Yuan C, Chang F-C, Dai L (2013) Synthesis, characterization and self-assembly of hybrid pH-sensitive block copolymer containing polyhedral oligomeric silsesquioxane (POSS). *React Funct Polym* 73:1646–1655
15. Chu C-C, Tsai Y-J, Hsiao L-C, Wang L (2011) Controlled self-aggregation of C<sub>60</sub>-anchored multiarmed polyacrylic acids and their cytotoxicity evaluation. *Macromolecules* 44:7056–7061
16. Reynhout IC, Cornelissen JJLM, Nolte RJM (2009) Synthesis of polymer-biohybrids: from small to giant surfactants. *Acc Chem Res* 42:681–692
17. Hamley IW, Castelletto V (2017) Self-assembly of peptide bioconjugates: selected recent research highlights. *Bioconjug Chem* 28:731–739
18. Luo Q, Hou CX, Bai YS, Wang RB, Liu JQ (2016) Protein assembly: versatile approaches to construct highly ordered nanostructures. *Chem Rev* 116:13571–13632
19. Yang G, Zhang X, Kochovski Z, Zhang YF, Dai B, Sakai FJ, Jiang L, Lu Y, Ballauff M, Li XM, Liu C, Chen GS, Jiang M (2016) Precise and reversible protein-microtubule-like structure with helicity driven by dual supramolecular interactions. *J Am Chem Soc* 138:1932–1937
20. Yang G, Wu LB, Chen GS, Jiang M (2016) Precise protein assembly of array structures. *Chem Commun* 52:10595–10605
21. Börner HG (2009) Strategies exploiting functions and self-assembly properties of bioconjugates for polymer and materials sciences. *Prog Polym Sci* 34:811–851
22. He N, Lu S, Zhao W, Du X, Huang S, Wang R (2014) Fabrication of the self-assembly systems based on protein molecules. *Prog Chem* 26:303–309
23. Maassen SJ, van der Ham AM, van der Cornelissen JJLM (2016) Combining protein cages and polymers: from understanding self-assembly to functional materials. *ACS Macro Lett* 5:987–994
24. Le Droumaguet B, Velonia K (2008) In situ ATRP-mediated hierarchical formation of giant amphiphile bionanoreactors. *Angew Chem Int Ed* 47:6263–6266
25. Reynhout IC, Cornelissen JJLM, Nolte RJM (2007) Self-assembled architectures from biohybrid triblock copolymers. *J Am Chem Soc* 129:2327–2332
26. Kadir MA, Lee C, Han HS, Kim B-S, Ha E-J, Jeong J, Song JK, Lee S-G, An SSA, Paik H (2013) In situ formation of polymer–protein hybrid spherical aggregates from (nitrotriacetic acid)-end-functionalized polystyrenes and His-tagged proteins. *Polym Chem* 4:2286–2296
27. Velonia K, Rowan AE, Nolte RJM (2002) Lipase polystyrene giant amphiphiles. *J Am Chem Soc* 124:4224–4225
28. Thomas CS, Xu L, Olsen BD (2013) Effect of small molecule osmolytes on the self-assembly and functionality of globular protein–polymer diblock copolymers. *Biomacromolecules* 14:3064–3072
29. Lam CN, Yao H, Olsen BD (2016) The effect of protein electrostatic interactions on globular protein–polymer block copolymer self-assembly. *Biomacromolecules* 17:2820–2829
30. Lam CN, Yao H, Olsen BD (2012) Kinetically controlled nanostructure formation in self-assembled globular protein–polymer diblock copolymers. *Biomacromolecules* 13:2781–2792
31. Liu Z, Dong C, Wang X, Wang H, Li W, Tan J, Chang J (2014) Self-assembled biodegradable protein–polymer vesicle as a tumor-targeted nanocarrier. *ACS Appl Mater Interfaces* 6:2393–2400
32. Wei KC, Li J, Chen GS, Jiang M (2013) Dual molecular recognition leading to a protein–polymer conjugate and further self-assembly. *ACS Macro Lett* 2:278–283
33. Han GD, Wang J-T, Ji XT, Liu L, Zhao HY (2017) Nanoscale proteinosomes fabricated by self-assembly of a supramolecular protein–polymer conjugate. *Bioconjug Chem* 28:636–641
34. Jang Y, Champion JA (2016) Self-assembled materials made from functional recombinant proteins. *Acc Chem Res* 49:2188–2198
35. Obermeyer AC, Bradley DO (2015) Synthesis and application of protein-containing block copolymers. *ACS Macro Lett* 4:101–110
36. Dong CH, Liu ZY, Wang S, Zheng B, Guo WS, Yang WT, Gong XQ, Wu XL, Wang HJ, Chang J (2016) A protein–polymer bioconjugate-coated upconversion nanosystem for simultaneous tumor cell imaging, photodynamic therapy, and chemotherapy. *ACS Appl Mater Interfaces* 8:32688–32698
37. He N, Lu Z, Zhao W (2015) pH-responsive double hydrophilic protein–polymer hybrids and their self-assembly in aqueous solution. *Colloid Polym Sci* 293:3517–3526
38. He N, Wang Y, Lu Z (2016) Temperature-responsive “tadpole-shaped” protein–polymer hybrids and their self-assembly behavior. *Polym Adv Technol* 27:1376–1382
39. Pelegri-O’Day EM, Maynard HD (2016) Controlled radical polymerization as an enabling approach for the next generation of protein–polymer conjugates. *Acc Chem Res* 49:1777–1785

40. Ashford EJ, Naldi V, O'Dell R, Billingham NC, Armes SP (1999) First example of the atom transfer radical polymerisation of an acidic monomer: direct synthesis of methacrylic acid copolymers in aqueous media. *Chem Commun* (14):1285–1286. doi:[10.1039/A903773J](https://doi.org/10.1039/A903773J)
41. Wang Y, He N, Lu Z (2017) Synthesis of end-functional and mid-functional temperature-responsive poly (*N,N*-diethyl-acrylamide) by ATRP. *Acta Polym Sin* 3:464–470
42. Hasneen A, Cho I, Kim K-W, Paik H (2012) Synthesis of poly(ethylene glycol)-*b*-poly(mercapto ethylacrylamide) diblock copolymer via atom transfer radical polymerization. *Polym Bull* 68:681–691
43. Lele BS, Murata H, Matyjaszewski K, Russell AJ (2005) Synthesis of uniform protein–polymer conjugates. *Biomacromolecules* 6:3380–3387
44. Spicer CD, Davis BG (2014) Selective chemical protein modification. *Nat Commun* 5:4740–4753
45. Boutoureira O, Bernardes GJL (2015) Advances in chemical protein modification. *Chem Rev* 115:2174–2195
46. Matsumoto NM, Prabhakaran P, Rome LH, Maynard HD (2013) Smart vaults: thermally-responsive protein nanocapsules. *ACS Nano* 7:867–874
47. Lavigneur C, Hendriks L, Hoogenboom R, Cornelissen JJLM, Nolte RJM (2011) Thermoresponsive giant biohybrid amphiphiles. *Polym Chem* 2:333–340
48. Wang X, Duan Y, Li C, Lu Y (2015) Synthesis, self-assembly, and formation of polymer vesicle hydrogels of thermoresponsive copolymers. *J Mater Sci* 50:3541–3548
49. Liu G-Y, Chen C-J, Ji J (2012) Biocompatible and biodegradable polymersomes as delivery vehicles in biomedical applications. *Soft Matter* 8:8811–8821
50. Wang H, Zhang M, Ni P, He J, Hao Y, Wu Y (2013) Synthesis of pH-responsive amphiphilic diblock copolymers containing polyisobutylene via oxyanion-initiated polymerization and their multiple self-assembly morphologies. *Chin J Polym Sci* 31:218–231
51. Du J, O'Reilly RK (2009) Advances and challenges in smart and functional polymer vesicles. *Soft Matter* 5:3544–3561